Semina Ciências Exatas e Tecnológicas

e-ISSN 1679-0375
ARCHAEOMETRY

ORIGINAL ARTICLE DOI 10.5433/1679-0375.2025.v46.52849

iThenticate

Non-Destructive Characterization of a Crucifix by X-Ray Fluorescence and Digital Radiography

Caracterização não Destrutiva de um Crucifixo por Fluorescência de Raios X e Radiografia Digital

Anderson Gomes de Paula[1], Isis Verona Nascimento da Silva Franzi[1], Josiane Emerich Cavalcante[2], Roberta Manon de Paula Sales Borges[2], Rafael Azevedo Fontenelle Gomes[3], Fernando Cordeiro Barbosa Gonçalves[4], Marcos Vinicius Vieira Coutinho [5], Davi Ferreira de Oliveira[6], Ricardo Tadeu Lopes[6]

Received: April 25, 2025 *Received in revised form: August 29, 2025* *Accepted: October 17, 2025* *Available online: November 28, 2025*

ABSTRACT

This study analyzes an 18th/19th-century crucifix from the sacristy of the Church of Santa Luzia, Rio de Janeiro, through X-Ray Fluorescence (XRF) and Digital Radiography (DR). The investigation aimed to identify the elemental composition of pigments and assess the structural condition of the sculpture. XRF revealed elements such as calcium, lead, and mercury, indicating historical pigments like calcium carbonate, lead white, and vermilion. The presence of lithopone and phthalocyanine materials introduced in the late 19th century suggests later repainting. DR imaging exposed structural issues including flaking, cracks, and hidden metallic components such as the halo, *titulus crucis*, and nails. Internal features like joints and fixations were also identified, enhancing understanding of fabrication and conservation needs. The results demonstrate the relevance of atomic techniques for cultural heritage preservation, providing essential data for conservation planning. The artwork belongs to the collection of IPHAN (Brazilian National Institute of Historic and Artistic Heritage).

keywords sacred crucifix, X-ray fluorescence, digital radiography, historical pigments, heritage conservation

RESUMO

Este estudo analisa um crucifixo dos séculos XVIII/XIX, proveniente da sacristia da Igreja de Santa Luzia, no Rio de Janeiro, por meio de Fluorescência de Raios X (XRF) e Radiografia Digital (DR). A investigação teve como objetivo identificar a composição elementar dos pigmentos e avaliar o estado estrutural da escultura. A XRF revelou elementos como cálcio, chumbo e mercúrio, indicando pigmentos históricos, como carbonato de cálcio, branco de chumbo e vermelhão. A presença de litopone e materiais à base de ftalocianina, introduzidos no final do século XIX, sugere repinturas posteriores. As imagens radiográficas evidenciaram problemas estruturais, como lascamentos, fissuras e componentes metálicos ocultos, incluindo o halo, o *titulus crucis* e os pregos. Também foram observadas características internas, como junções e fixações, ampliando a compreensão sobre a fabricação e a conservação da peça. Os resultados demonstram a relevância das técnicas atômicas na preservação do patrimônio cultural. A obra integra o acervo do IPHAN (Instituto do Patrimônio Histórico e Artístico Nacional).

palavras-chave crucifixo sacro; fluorescência de raios X; radiografia digital; pigmentos históricos; conservação do patrimônio

[1]Dr., LIN/COPPE, UFRJ, Rio de Janeiro, Brazil. eng.agp@gmail.com, isisfranzi@gmail.com
[2]M.Sc., LIN/COPPE, UFRJ, Rio de Janeiro, Brazil. emerichcavalcante@gmail.com, robertamanon2009@gmail.com
[3]M.Sc., National Institute of Historic and Artistic Heritage (IPHAN), Brazil. o.raffael@gmail.com
[4]M.Sc., School of Fine Arts, UFRJ, Brazil. fernandocbgoncalves95@gmail.com
[5]M.Sc., Graduate Program in History, PPHPBC/FGV Rio de Janeiro, Brazil. mvcout@gmail.com
[6]Prof. Dr., LIN/COPPE, UFRJ, Rio de Janeiro, Brazil. davifoliveira@coppe.ufrj.br, rlopes@coppe.ufrj.br

Introduction

The analysis of the religious sculpture *Crucifix of the Sacristy* was carried out in the Church of Santa Luzia, in Rio de Janeiro. The piece, dated between the 18th and 19th centuries, presents formal and stylistic characteristics consistent with sacred sculptures from this period, made of carved, gilded, and polychromed wood.

In Catholic tradition, the crucifix is the principal symbol of the Passion and Redemption of Christ, serving as an object of devotion and artistic expression throughout the centuries. Its representation evolved from a symbolic form to one seeking naturalism and human expression, particularly from the Renaissance onward (Adam, 2021; Campos, 2015; Frade, 2016).

The production of such sculptures involved complex stages, including wood preparation, the application of animal glue and gypsum as a base, and the use of Armenian bole for gilding, composed of iron oxides and other mineral elements. These layers received historical pigments such as lead white, vermilion, and calcium carbonate, widely documented in coeval artworks (Barata, 2015; Hradil et al., 2017; Laurie, 1967; Lins et al., 2020).

The scientific characterization of sacred artworks has benefited from the use of non-destructive techniques such as X-Ray Fluorescence (XRF) and Digital Radiography (DR), which allow the identification of elemental composition, the assessment of structural integrity, and the documentation of the conservation state of sculptures (Borges et al., 2025; Cavalcante et al., 2025; Oliveira et al., 2023; Silveira & Falcade, 2022).

The combination of these approaches provides essential information for conservation planning and the appreciation of historical and artistic heritage. The objectives of this study are:

(i) to characterize the elemental composition of the pigments in the religious crucifix sculpture;
(ii) to assess its structural integrity through the combined application of XRF and DR;

(iii) to identify possible interventions or evidence of the manufacturing process.

Material and methods

The study examines a large religious sculpture representing a sacristy altar crucifix in the form of a Latin cross. Crafted from carved, gilded, and polychromed wood, the artwork exhibits stylistic and material characteristics consistent with pieces produced between the 18th and 19th centuries. Figure 1 presents the *Crucifix of the Sacristy* and the delimited area selected for analysis.

Figure 1 - *Crucifix of the Sacristy* with delimited area of analysis.

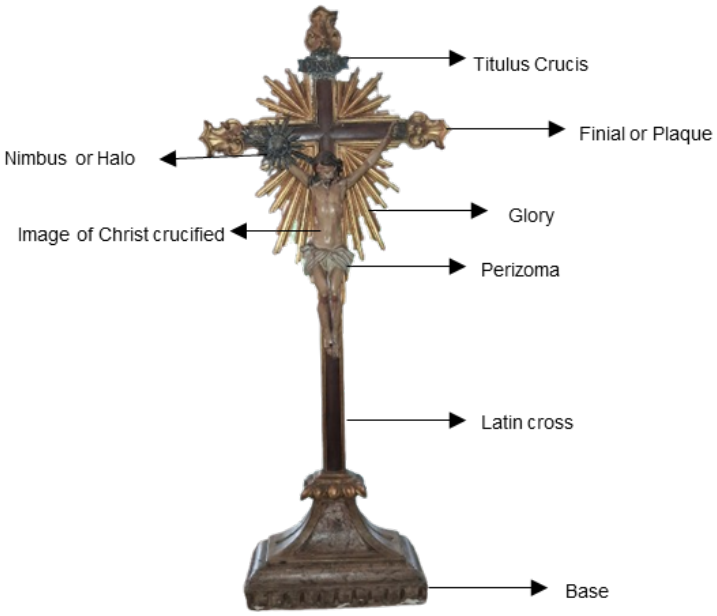

As complementary adornments, the crucifix includes separate attributes made of a silver alloy, among which are:

(i) the *titulus crucis*, a metallic plaque bearing the inscription "INRI," affixed to the top of the central arm of the cross;

(ii) the nimbus or radiance, a ray-shaped disc supported by a rod that extends from the back of Christ and hovers above the upper part of His head.

The dimensions of the artwork are presented in Table 1.

Table 1 - Dimensions of the Crucifix sculpture.

Component	Height (cm)	Width (cm)	Depth (cm)
Cross	110.3	47.5	12.5
Christ	39.5	28.0	8.5
Base (rectangular)	21.0	33.4	12.5

The voltage parameters used for radiography were determined experimentally *in situ*, considering the variable thickness of the sculpture. A voltage of $90\,\text{kV}$ was applied specifically to the base, due to its greater thickness, while the other regions were radiographed at $70\,\text{kV}$, providing better image contrast and quality.

A portable and compact X-ray tube, model ICM CP120B (Teledyne ICM, 2023),was employed. The equipment weighs $7.5\,\text{kg}$ and operates with a maximum voltage of $120\,\text{kVp}$ (minimum current: $0.1\,\text{mA}$) and a minimum voltage of $40\,\text{kVp}$ (maximum current: $1.0\,\text{mA}$).

The source-to-detector distance (SDD) was fixed at $1500\,\text{mm}$, below which the radiographic images were acquired. The detector was supported by an aluminum stand developed at the LIN (Laboratory of Nuclear Instrumentation).

The equipment features a focal spot size of $1\,\text{mm}$ and can be operated either by battery or connected to the electrical grid. It is remotely controlled via a $30\,\text{m}$ trigger cable, which allows operation under safe conditions.

Detection was performed using a flat-panel detector, model DXR 250U-W (General Electric – GE), responsible for signal detection and initial image processing. The detector has an active area of $400\,\text{mm} \times 400\,\text{mm}$, a physical pixel size of $200\,\mu\text{m}$, a thickness of $26\,\text{mm}$, and an approximate weight of $5\,\text{kg}$. The radiographs produce full-format images up to 2048×2048 pixels, allowing visualization of structural details such as cracks and inclusions.

The application of the DR technique was divided into three stages, using different voltages ($70\,\text{kV}$ and $90\,\text{kV}$), a current of $1\,\text{mA}$, and exposure times of $5\,\text{s}$ per frame. Each radiograph consisted of capturing five frames per position, ensuring greater sharpness and reduced noise.

For the acquisition of the crucifix's digital radiographs, images were captured in different sections and heights due to the detector's limited size. In total, nine images were obtained, organized into three main sections: upper, middle, and lower. These sections were carefully edited and digitally combined, resulting in a single reconstructed image that preserves the object's internal details without compromising data integrity.

Two non-destructive techniques were applied: Digital Radiography (DR), performed on the entire artwork, and X-Ray Fluorescence (XRF), through multiple-point analyses distributed across the surface of the sculpture, as shown in Figure 2.

For the pigment analysis of the sculpture, Figure 2(a), 22 XRF measurements were carried out using a portable commercial Bruker Tracer III-SD spectrometer. The equipment is equipped with a Rh anode X-ray tube and a Si-PIN diode detector, operating at $40\,\text{kV}$ and $35\,\mu\text{A}$. The acquisition time for each analyzed point was $60\,\text{s}$.

Results and Discussion

X-Ray Fluorescence Analysis

The XRF spectra were processed using Artax (Bruker) for elemental identification and Origin for graphical presentation. The sculpture shows visible deterioration, including chipped regions, paint loss, and fractures, Figure 3.

Figure 2 - *Crucifix of the Sacristy*: (a) XRF analysis points, and (b) crucifix without marked points.

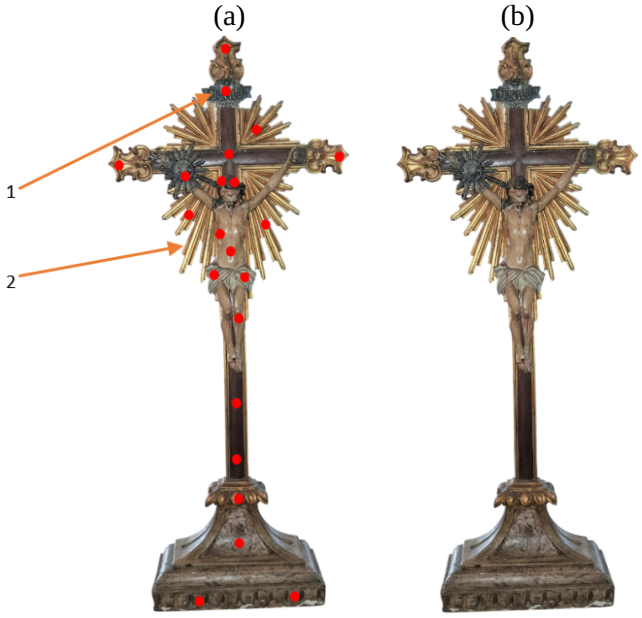

Figure 3 - Images of chipped or degraded areas of the crucifix: (a) frontal view showing flaking on the torso; (b) lateral view with deterioration near the arms; (c) lower section with surface degradation and color fading; (d) close-up of the head showing cracks and paint loss.

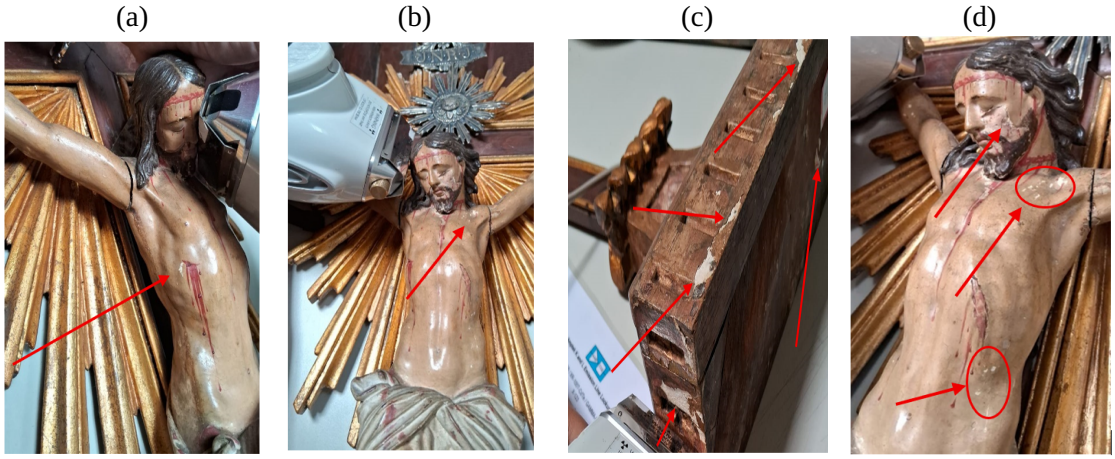

The areas indicated, Figures 3(a)-(d), correspond to distinct structural components, each with specific liturgical and iconographic significance, which justified their individual analysis by XRF and DR. This mapping was also essential for consistent documentation and future comparative studies.

Background signals of rhodium (Rh), argon (Ar), and nickel (Ni) were attributed to the X-ray tube and instrument structure, unrelated to the object. The spectra revealed significant peaks of calcium (Ca) and lead (Pb), suggesting a uniform preparatory layer composed of gypsum and lead white, traditionally mixed with diluted animal glue to create a reflective surface enhancing the brilliance of overlying colors (Mayer, 2006; Miu & Niculescu, 2022; Slotsgaard et al., 2024).

These elements were detected not only in white areas but also across flesh tones, hair, and the crucifix shaft, confirming their use as components of the underlying preparation layer.

In XRF spectra, variations in peak intensity are expected depending on the analyzed region. Comparing the relative intensities of elemental peaks is fundamental for inferring pigment composition and identifying possible mixtures. For instance, the simultaneous occurrence of intense Pb (lead) and Hg (mercury) peaks suggests the combined use of lead white and vermilion, responsible for pinkish or orange hues. Such interpretation goes beyond the mere detection of individual elements, requiring the evaluation of intensity ratios, peak overlaps, and potential matrix effects to accurately characterize the pigments present.

Figure 4 illustrates the elemental distribution in the analyzed areas.

Figure 4 - XRF spectra of selected analyzed regions: (a) drop of blood on the chest, (b) leg region, (c) perizoma, (d) hair, (e) shaft of the Crucifix of the Sacristy (lower part), (f) shaft of the Crucifix of the Sacristy (upper part), and (g) metallic radiance.

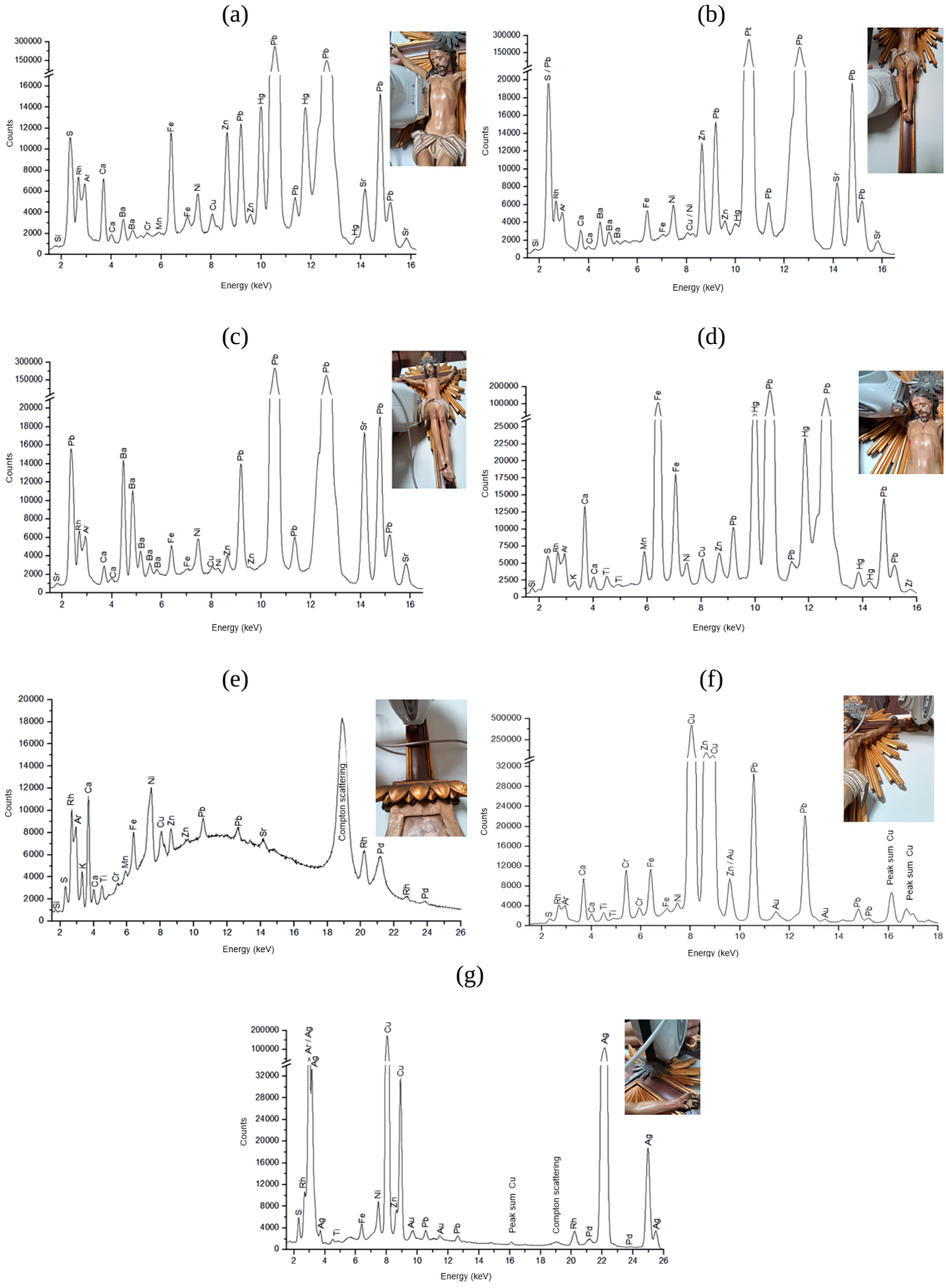

Red

The XRF analysis detected barium and zinc, suggesting the use of lithopone and/or zinc white in the eighteenth-century artwork. The presence of lithopone indicates possible later restorations, as this pigment was introduced only at the end of the nineteenth century, whereas zinc white, available since 1835, may belong to the original paint layer.

Barium occurrence deserves attention, as it may indicate lithopone or the use of barium sulfate as a filler commonly applied in both historical and modern paint formulations to increase opacity, stabilize color, and improve cohesion of the pictorial layer (Buyondo et al., 2025). The chemical similarity between barium and calcium, both alkaline earth elements, supports this interpretation. Thus, the co-detection of Ba with elements such as Zn or Ti may reflect stratigraphic or filler origins rather than direct pigment correlations.

Calcium peaks confirm the use of calcium carbonate, gypsum, and bone white. Titanium was detected only in trace amounts, as observed in spectra, see Figures 4(d)-(f), corresponding to brownish areas. This indicates that Ti is likely related to mineral impurities in iron oxides used in the polychromy rather than intentional use of titanium white (Grygar et al., 2003).

Strong mercury (Hg) peaks indicate vermilion in red-painted regions, while lead (Pb) peaks in the same spectra see Figures 4(a)-(f), suggest the use of lead white mixed with red pigment to adjust tonal intensity. Some Pb may also derive from the preparatory layer, a common historical practice. The predominance of Pb in red areas further supports the presence of red lead-based pigments, such as litharge and red lead, widely documented in sacred polychromies from the seventeenth to nineteenth centuries (Gettens & Stout, 1966).

Iron (Fe) detection reinforces the possible use of red ochre as a complementary pigment. Other detected elements appeared only in trace levels, not significantly affecting chromatic definition. Recent studies confirm the recurrent presence of lead-based reds—especially red lead and litharge—in sacred artworks from the same period, due to their stability and strong tinting power (Shen et al., 2024).

Flesh Tones

The region encompassing the nail, arm, and leg of Christ exhibits a beige hue consistent with a mixture of white, yellow, red, and brown pigments. This interpretation is supported by the simultaneous detection of barium, zinc, lead, iron, and mercury elements typically associated with white, yellow, brown, and red pigments. The presence of barium and zinc suggests the use of lithopone or zinc white with traces of barium.

Since lithopone was only introduced in the late 19th century and the crucifix dates from the 18th–19th centuries, the pigment's detection indicates possible later restorations. This hypothesis aligns with the historical timeline of lithopone's availability and potential repaintings long after the original execution.

Red pigments containing lead, iron, and mercury likely correspond to litharge, red lead, red ochre, and vermilion, whereas yellow pigments may include yellow ochre and massicot. Brown hues can be attributed to brown ochre and sienna, Figure 4(b).

The detection of strontium (Sr) may indicate strontium yellow (ColourLex, 2025; Otero et al., 2017). However, due to the low peak intensity, Sr is more plausibly related to celestine, a mineral commonly found in gypsum-bearing rocks (Franceschi & Locardi, 2014) rather than intentional pigment use (Bitossi et al., 2005).

White

The coexistence of barium and zinc detected in the spectra indicates the possible presence of lithopone, while the identification of zinc also suggests the use of zinc white. Intense lead (Pb) peaks confirm the presence of lead white, consistent with historical practices that employed calcium carbonate or gypsum in preparatory layers of sculptures (Alves, 1989; Nunes, 1615).

The variation in intensity between Pb and Ca peaks can be attributed to the attenuation effect of lead on incident X-rays, which reduces radiation interaction with the underlying calcium-based layer, Figure 4(c).

Brown

The brown areas analyzed on the crucifix include the base, Christ's hair, and the shaft, with multiple measurement points in each. A separate subsection for yellow pigments was not created, as no pure yellow tones were identified in the artwork; in this case, pigments such as chrome yellow and zinc yellow appear only as components of mixtures that produced brown or beige hues.

In the base, the most intense XRF signals correspond to calcium (Ca), iron (Fe), zinc (Zn), and lead (Pb), with traces of copper (Cu) and chromium (Cr), suggesting a mixture of white pigments with ochres and colors such as chrome yellow, zinc yellow, and blue pigments (azurite, Prussian blue, phthalocyanine blue), whose combination can result in brown tones. In the hair of the sculpture, the main detected elements were iron (Fe), mercury (Hg), and lead (Pb), with smaller amounts of calcium (Ca), manganese (Mn), and copper (Cu), indicating a distinct formulation possibly involving vermilion, umber, ochres, and blue pigments such as azurite and phthalocyanine.

The visual presence of brown in these areas and its chemical occurrence indicate that it may have been used as a component in mixtures to obtain flesh tones, a common practice in historical polychromies in which blue and green pigments were sometimes incorporated in small quantities to adjust the final hue.

X-ray scattering along the shaft occurs due to the absence of a pictorial layer, causing the radiation to interact directly with the wood. Because wood has a low atomic number, it favors scattering over the photoelectric effect, resulting in a spectrum dominated by continuous signals and making the identification of specific elemental peaks more difficult.

Iron (Fe) and manganese (Mn) indicate the presence of ochre and umber pigments. Copper (Cu), palladium (Pd), and chromium (Cr) may originate from a nearby metallic alloy.

Calcium (Ca) probably corresponds to a preparatory layer, while titanium (Ti) and strontium (Sr) are likely impurities from gypsum. Zinc (Zn) suggests the use of zinc white, Figures 4(d)–(f).

Gold

The XRF spectra of the gilded areas reveal intense peaks of calcium (Ca), copper (Cu), zinc (Zn), and lead (Pb), followed by chromium (Cr) and iron (Fe), while other elements were detected only in trace amounts. The presence of iron (Fe) indicates the use of Armenian bole, a type of clay rich in iron oxides, traditionally selected for gilding because of its fine particle size and reddish color, which enhances the warm tone of the gold leaf (Barata, 2015; Hradil et al., 2003, 2017). The XRF analysis also identified elements likely originating from the clay present in the sculpture, such as silicon (Si), calcium (Ca), titanium (Ti), and iron (Fe) (Le Gac et al., 2014).

It should be noted that XRF analysis alone does not allow definitive confirmation of the presence of Armenian bole. Complementary techniques such as Scanning Electron Microscopy coupled with Energy-Dispersive Spectroscopy (SEM-EDS), X-ray Diffraction (XRD), or stratigraphic cross-section studies would be required to mineralogically characterize the preparatory material.

The presence of lead (Pb) and chromium (Cr) suggests the use of chrome yellow in the sculpture. According to Sandu et al. (2011), chrome yellow was applied beneath gold leaf in gilding techniques to improve adhesion and to enhance the brilliance of the surface with a warm and radiant background.

Chrome yellow, or lead chromate, can vary in hue from lemon-yellow to orange, depending on particle size and precipitation conditions. Although its use is documented since the early 19th century, it remains uncertain whether it was employed as an underlayer for gold leaf or as a substitute for gold, as suggested by similar studies (Sansonetti et al., 2020).

The detection of gold (Au) confirms the use of gold leaf in the gilded areas (Mastrotheodoros & Beltsios, 2022). However, the high intensity of copper (Cu) peaks compared to those of gold (Au) indicates that the gilding was executed with a copper-based alloy leaf containing a low proportion of gold, Figure 4(f) and 4(g).

Based on the XRF analysis, Table 2 lists the possible pigments that compose the crucifix's polychromy (Bassett & Alvarez, 2011; Clark, 2002; Feller, 1986, 1993; Fitzhugh, 1997; Gliozzo & Ionescu, 2022; Grygar et al., 2003).

Table 2 - List of possible pigments used in the polychromy, with their main elements, color, composition, and period of use.

Key Elements	Pigment	Color	Composition	Period of use
Ba / S / Zn	Lithopone	white	$ZnS + BaSO_4$	1874 / still in use
Ca	Calcium carbonate (chalk, calcite)	white	$CaCO_3$	Antiquity / still in use
Ca	Gypsum	white	$CaSO_4 \cdot 2H_2O$	Antiquity / still in use
Ca	Bone white	white	$Ca_3(PO_4)_2$	Antiquity / still in use
Pb	Lead white (lead carbonate, cerussite)	white	$2PbCO_3 \cdot Pb(OH)_2$	Antiquity / 20th century
Ti	Titanium dioxide (titanium white)	white	TiO_2	1910–1920 / still in use
Zn	Zinc white	white	ZnO	1835 / still in use
Fe	brown ochre	brown	Fe_2O_3 + clay + silica	Prehistory / still in use
Fe	sienna	brown	Fe_2O_3	Antiquity / still in use
Fe / Mn	Umber	brown	$Fe_2O_3 \cdot MnO_2$	Prehistory / still in use
Cr	Chrome yellow	yellow	$PbCrO_4 \cdot PbSO_4$	19th century / still in use
Zn / Cr	Zinc yellow	yellow	$ZnCrO_4$	19th century / still in use
Fe	Yellow ochre	yellow	$Fe_2O_3 \cdot H_2O$ + clay + silica	Prehistory / still in use
Pb	Massicot	yellow	PbO	Antiquity / up to 20th century
Sr / Cr	Strontium yellow	yellow	$SrCrO_4$	19th century / still in use
Fe	Red ochre	red	$Fe_2O_3 \cdot H_2O$ + clay + silica	Prehistory / still in use
Hg / S	Vermilion	red	HgS	Antiquity / up to 19th century
Pb	Litharge	red	PbO	Antiquity / up to 20th century
Pb	Red lead	red	Pb_3O_4	Up to 20th century
Cu / Cl	Phthalocyanine green	green	$Cu(C_{32}H_{16-n}Cl_nN_8)$	1938 / still in use
Cu	Azurite (Copper(II))	blue	$2CuCO_3 \cdot Cu(OH)_2$	Antiquity / 18th century
Cu	Phthalocyanine blue	blue	$Cu(C_{32}H_{16}N_8)$	1930 / still in use
Fe	Prussian blue	blue	$Fe_4[Fe(CN)_6]_3 \cdot 14–16H_2O$	1704 / still in use

Digital Radiography (DR)

The radiographic analysis made it possible to identify relevant aspects of the internal structure and conservation state of the crucifix. Nails were detected in the base, as well as joints connecting Christ's arms to the torso, and metallic elements fixing the hands and feet to the cross. Damage was also observed at the right extremity of the piece, possibly resulting from wear or handling over time. The preservation of original silver adornments, such as the radiant halo and the *titulus crucis*, was confirmed, both remaining intact.

These results provide detailed information regarding both the technical process and the insights obtained from the artwork. From a technical standpoint, the strategy of acquiring nine segmented radiographs followed by digital editing and reconstruction successfully overcame the detector size limitation, producing a high-definition final image that preserved sharpness and data integrity.

With respect to the sculpture itself, the images revealed its internal composition, joining and fastening points, damaged areas, and the integrity of original decorative elements. Together, these findings offer objective support for understanding its structural configuration and for planning future conservation actions. Figures 5(a) and 5(b) show the finalized digital radiograph; blue circles indicate the junctions, and red arrows denote nails and spikes.

Figure 5 - Digital radiography: (a) system; (b) the *Crucifix of the Sacristy*, where ▬ indicates metal (nails), ▬ marks joints, and ▬ highlights the halo and *titulus crucis*.

(a) (b)

To the naked eye, the joints of Christ's arms can be observed in Figure 6(a), indicated by blue arrows. However, in the case of the crucifix, the wooden joints are not externally visible. Only through the radiographic images was it possible to identify the presence of joints within the wooden structure of the crucifix, Figure 6(b), indicated by red arrows.

Figure 6 - Upper part of the crucifix: (a) photograph, (b) radiograph.

(a) (b)

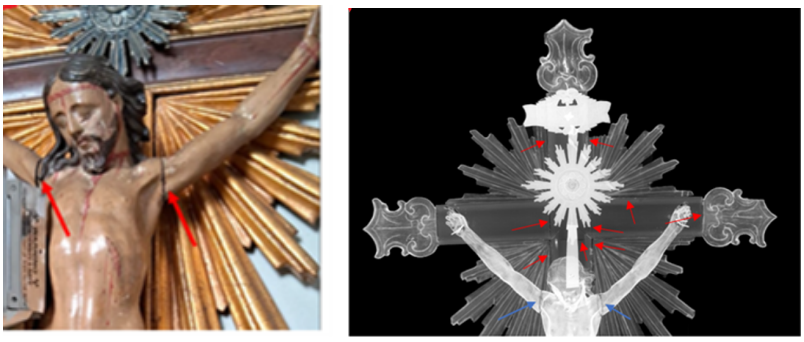

Small nails (indicated by red arrows) can be identified at the junction of the main shaft of the crucifix, joining the larger wooden component to a smaller finishing piece, Figure 7. In addition, there appears to be a possible material loss in the region of the index and little fingers of the left hand, Figure 7(a), highlighted by red circles, as well as in the index finger and palm of the right hand of the sculpture, Figure 7(b).

It is also observed that no nails are visible fixing the finishing piece to the main shaft of the crucifix, suggesting that this part may have been attached by fitting or gluing.

Some irregularities or areas of reduced density may indicate defects in the wood or disintegration of the pictorial layers. The irregular distribution of bright areas observed in the radiograph may reflect several factors related to the painted layers and the application of pigments. Among these factors, the pictorial techniques employed by the artist stand out, as they may have resulted in variations in the thickness or density of the paint.

In addition, certain regions may show a greater accumulation of lead white, used to create volumetric effects or to emphasize specific elements of the image. It is also important to consider the possibility of later retouching's in specific areas of the painting, which may have contributed to variations in the radiopacity of these regions, particularly noticeable in the arms and hands, Figure 8.

Figure 7 - Radiograph of the hands of the crucified Christ: (a) left hand (radiograph), (b) right hand (radiograph).

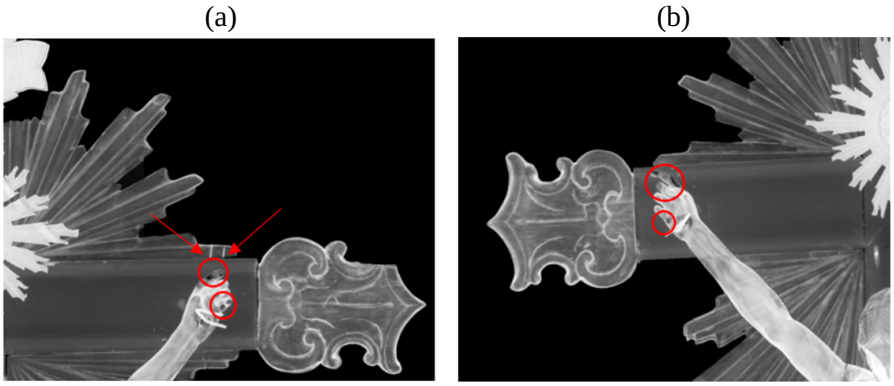

Figure 8 - Radiograph of the arms of the crucified Christ. (a) right arm (radiograph), (b) left arm (radiograph).

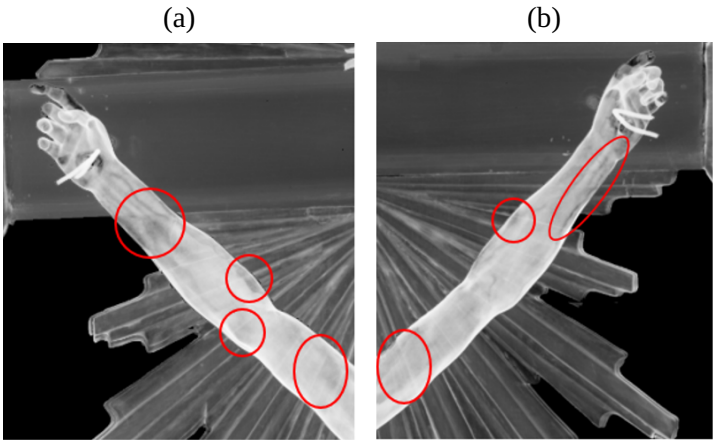

In the central region of the crucifix, it is possible to observe the wire used to fix and support the suspended sculpture, Figure 9, indicated by red arrows.

Figure 9 - Central region of the crucifix.

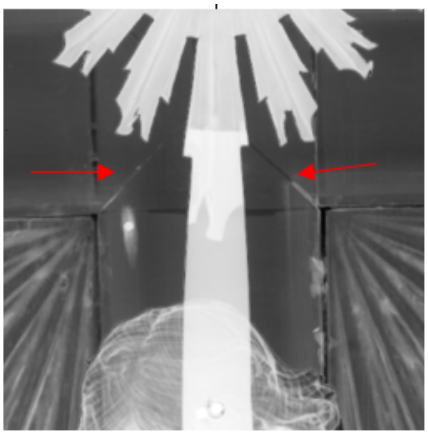

The suspension wire present in the figure of Christ is related to the fixation and stability of the sculpture, allowing the image to be properly maintained in its position. In the specific case of this crucifix, classified as a “standing crucifix”, the piece includes a pedestal support (*peanha*) (Moutinho et al., 2011).

This suspension feature is not exclusive to this artwork; it is also found in other devotional images, especially those designed for liturgical use in sacristies and altars, where both the stability of the piece and the possibility of display in different contexts were desired.

Conclusion

The study of the *Crucifix of the Sacristy* from the Church of Santa Luzia revealed valuable information about its composition, state of preservation, and historical context. X-ray fluorescence (XRF) identified traditional pigments such as calcium carbonate, gypsum, lead white, zinc white, vermilion, and ochres, consistent with 18th–19th century artistic practices. The detection of lithopone and possible phthalocyanine pigments indicates later restorations or repainting.

Digital radiography (DR) complemented the analysis by exposing internal fractures, fissures, and structural heterogeneities resulting from aging or previous interventions. The integration of both techniques proved essential for distinguishing original materials from later additions and for assessing the sculpture's structural integrity.

Overall, this multidisciplinary approach contributes to understanding the materials and techniques of Brazilian sacred art and supports future conservation efforts aimed at preserving its historical and artistic value.

Acknowledgments

This study was supported by the Brazilian National Council for Scientific and Technological Development (CNPq), INCT_INAIS (grant 424498/2025-1), and was partially funded by the Coordination for the Improvement of Higher Education Personnel (CAPES) – Finance Code 001. The authors would also like to thank the Rio de Janeiro State Research Support Foundation (FAPERJ) for their financial support.

Author Contributions

A. G. Paula participated in: Conceptualization, Data Curation, Formal Analysis, Investigation, Methodology, Visualization, Writing – original draft. **I. V. N. S. Franzi**, **J. E. Cavalcante** participated in: Supervision, Validation, Visualization, Writing – review and editing. **R. M. P. S. Borges** participated in: Validation, Visualization, Investigation. **R. A. F. Gomes, F. C. B. Gonçalves**, **M. Coutinho** participated in: Resources, Investigation. **D. F. Oliveira** participated in: Validation, Supervision, Writing – review and editing. **R. T. Lopes** participated in: Resources, Funding.

Conflicts of Interest

The authors declare that they have no known competing financial interests or personal relationships that could have influenced the work reported in this paper.

References

Adam, K. (2021). *The Spirit of Catholicism*. Rare Treasure Editions. (Original work published in Portuguese).

Alves, N. (1989). *The Art of Wood Sculpture in Porto during the Baroque Period (Artists and Clients, Materials and Techniques)*. Arquivo Histórico. (Original work published in Portuguese).

Barata, C. S. S. (2015). *Materials and Polychromy Techniques in Scientific and Popular Baroque Carving from Northwestern Portugal* [Doctoral dissertation, University of Aveiro, Portugal]. (Original work published in Portuguese).

Bassett, J., & Alvarez, M.-T. (2011). Process and collaboration in a seventeenth-century polychrome sculpture: Luisa Roldán and Tomás de Losarcos. *Getty Research Journal*, *3*, 15–32. https://www.jstor.org/stable/23005385

Bitossi, G., Giorgi, R., Mauro, M., Salvadori, B., & Dei, L. (2005). Spectroscopic techniques in cultural heritage conservation: A survey. *Applied Spectroscopy Reviews*, *40*(3), 187–228. https://doi.org/10.1081/ASR-200054370

Borges, R., Franzi, Í., Cavalcante, J., Gusmão, E., Paula, A., Araújo, O., Lopes, R. T., & Oliveira, D. F. (2025). Non-destructive examination of a polychrome wooden sculpture from the 17th century. *Brazilian Journal of Radiation Sciences*, *12*(4A), 1–19. https://doi.org/10.15392/2319-0612.2024.2555

Buyondo, A. K., Kasedde, H., Kirabira, J. B., & Yusuf, A. A. (2025). Integration of Fillers in Paint Formulation: Comprehensive Insights into Methods, Properties, and Performance. *Results in Engineering*, *26*, 105543. https://doi.org/10.1016/j.rineng.2025.105543

Campos, A. A. (2015). A Cruz e Crucifixos em Acervos Mineiros. *Boletim do Ceib*, *19*(61), 1–6. https://www.eba.ufmg.br/boletimceib/index.php/boletimdoceib/article/view/93/76

Cavalcante, J. E., Borges, R. M. S. P., Franzi, I. V. N. S., Paula, A. G., Gomes, R. A. F., & Oliveira, D. F. (2025). Application of non-destructive techniques to evaluate the sculpture of Our Lady of Good Health. *The European Physical Journal Plus*, *140*, 586. https://doi.org/10.1140/epjp/s13360-025-06544-1

Clark, R. J. H. (2002). Pigment identification by spectroscopic means: an arts/science interface. *Comptes Rendus*, *5*(1), 7–20. https://doi.org/10.1016/S1631-0748(02)01341-3

ColourLex. (2025). Paintings, pigments used in their creation and scientific methods for the investigation of artworks. https://colourlex.com

Feller, R. L. (Ed.). (1986). *Artists' pigments: A handbook of their history and characteristics* (Vol. 1). Archetype Publications. https://www.nga.gov/content/dam/ngaweb/research/publications/pdfs/artists-pigments-vol1.pdf

Feller, R. L. (Ed.). (1993). *Artists' pigments: A handbook of their history and characteristics* (Vol. 2). Archetype Publications. https://www.nga.gov/content/dam/ngaweb/research/publications/pdfs/artists-pigments-vol2.pdf

Fitzhugh, E. (Ed.). (1997). *Artists' pigments: A handbook of their history and characteristics* (Vol. 3). Archetype Publications. https://www.nga.gov/content/dam/ngaweb/research/publications/pdfs/artists-pigments-vol3.pdf

Frade, G. D. S. (2016). *Between the Renaissance and the Baroque: The foundations of religious architecture and the Counter-Reformation – De Fabrica Ecclesiae, by Carlo Borromeo* [Doctoral dissertation, University of São Paulo]. (Original work published in Portuguese). https://doi.org/10.11606/T.16.2017.tde-16022017-093801

Franceschi, E., & Locardi, F. (2014). Strontium: A new marker of gypsum origin in cultural heritage? *Journal of Cultural Heritage*, *15*(5), 522–527. https://doi.org/10.1016/j.culher.2013.10.004

Gettens, R. J., & Stout, G. L. (1966). *Painting Materials: A Short Encyclopaedia*. Dover Publications. https://archive.org/details/paintingmaterial0000gett/page/n3/mode/2up

Gliozzo, E., & Ionescu, C. (2022). Lead-based white, red, yellow, and orange pigments and their alteration phases. *Archaeological and Anthropological Sciences*, *14*(1), 17. https://doi.org/10.1007/s12520-021-01407-z

Grygar, T., Hradilová, J., Hradil, D., Bezdicka, P., & Bakardjieva, S. (2003). Analysis of earth pigments in the backgrounds of Baroque paintings. *Analytical and Bioanalytical Chemistry*, *375*, 1154–1160. https://doi.org/10.1007/s00216-002-1708-x

Hradil, D., Grygar, T., Hradilová, J., & Bezdicka, P. (2003). Clay and iron oxide pigments in the history of painting. *Applied Clay Science*, *22*(5), 223–236. https://doi.org/10.1016/S0169-1317(03)00076-0

Hradil, D., Hradilová, J., Bezdicka, P., & Seredan, C. (2017). Late Gothic/Early Renaissance gilding technology and the traditional polishing material "Armenian bole": truly red clay or rather bauxite? *Applied Clay Science*, *135*, 271–281. https://doi.org/10.1016/j.clay.2016.10.004

Laurie, A. (1967). *The Painter's Methods and Materials*. Dover Publications.

Le Gac, A., Pessanha, S., & Carvalho, M. L. (2014). Application of energy-dispersive X-ray fluorescence spectrometry to polychrome terracotta sculptures from the Monastery of Alcobaça, Portugal. *Conservar Património*, *20*, 35–51. https://doi.org/10.14568/cp2014008

Lins, B. S., Gigante, G. E., Cesareo, R., Ridolfi, S., & Brunetti, A. (2020). Testing the accuracy of gold leaf thickness calculations using Monte Carlo simulations and MA-XRF scanning. *Applied Sciences*, *10*(10), 3582. https://doi.org/10.3390/app10103582

Mastrotheodoros, G. P., & Beltsios, K. G. (2022). Iron-based pigments: red, yellow, and brown ochres. *Archaeological and Anthropological Sciences*, *14*(2), 35. https://doi.org/10.1007/s12520-021-01482-2

Mayer, R. (2006). *The Artist's Handbook of Materials and Techniques*. Martins Fontes.

Miu, L., & Niculescu, M. (2022). Preliminary study on the adhesiveness properties of hide glue. *Revista de Pielarie Incaltaminte*, *22*, 2. https://doi.org/10.24264/lfj.22.2.7

Moutinho, S., Prado, R. B., & Londres, R. (2011). *Dicionário de Artes Decorativas & Decoração de Interiores*. Lexikon.

Nunes, F. (1615). *Arte da pintura, symmetria, e perspectiva*. Na officina de João Baptista Alvares. https://archive.org/details/artedapinturasym00nune/page/n3/mode/2up

Oliveira, R., Paula, A., Gonçalves, F., Sanches, F., Nardes, R., Santos, R., Azeredo, S., Araújo, O., Machado, A., Anjos, M., Lopes, R., & Oliveira, D. (2023). Analysis of a wooden statue using non-destructive X-ray techniques. *X-Ray Spectrometry*, *52*(6), 312–322. https://doi.org/10.1002/xrs.3327

Otero, V., Campos, M., Pinto, J., Vilarigues, M., Carlyle, L., & Melo, M. (2017). Barium, zinc, and strontium yellows in late 19th–early 20th century oil paintings. *Heritage Science*, *5*, 1–13. https://doi.org/10.1186/s40494-017-0160-3

Sandu, C. A., Sá, M. H., & Pereira, M. C. (2011). Ancient gilded art objects of the European cultural heritage: A review at different scales of characterization. *Surface and Interface Analysis*, *43*(8), 1134–1151. https://doi.org/10.1002/sia.3740

Sansonetti, A., Andreotti, A., Bertasa, M., Bonaduce, I., Corti, C., Facchin, L., La Nasa, J., Spiriti, A., & Rampazzi, L. (2020). Territory and related artworks: Stuccoworks from the Lombard lakes. *Journal of Cultural Heritage*, *46*, 382–398. https://doi.org/10.1016/j.culher.2020.06.009

Shen, L., Kang, Y., & Li, Q. (2024). Analytical study of polychrome clay sculptures in the Five-Dragon Taoist Palace of Wudang, China. *Coatings*, *14*(5), 540. https://doi.org/10.3390/coatings14050540

Silveira, S., & Falcade, T. (2022). Applications of energy-dispersive X-ray fluorescence in studies of metallic cultural heritage. *Journal of Cultural Heritage*, *57*, 243–255. https://doi.org/10.1016/j.culher.2022.09.008

Slotsgaard, T., Pastorelli, G., Buti, D., Scharff, M., & Andersen, C. (2024). Crack morphology and its correlation with ground materials used in paintings by Danish portrait painter Jens Juel. *Journal of Cultural Heritage*, *39*, 47–56. https://doi.org/10.1016/j.culher.2024.07.010

Teledyne ICM. (2023). *Home*. https://www.teledyneicm.com/